



# Impact of biopsy route, muscle pathway, and cortex target on safety and diagnostic yield in ultrasound-guided renal parenchymal biopsy

Kadir Han Alver<sup>1</sup>  
 Halil Serdar Aslan<sup>1</sup>  
 Muhammet Arslan<sup>1</sup>  
 Muhammed Tekinhatur<sup>2</sup>  
 Mahmut Demirci<sup>3</sup>  
 Nagihan Yalçın<sup>4</sup>  
 Ahmet Baki Yağcı<sup>1</sup>

<sup>1</sup>Pamukkale University Faculty of Medicine,  
Department of Radiology, Denizli, Türkiye

<sup>2</sup>Dicle University Faculty of Medicine, Department of  
Radiology, Diyarbakır, Türkiye

<sup>3</sup>Adnan Menderes University Faculty of Medicine,  
Department of Radiology, Aydın, Türkiye

<sup>4</sup>Pamukkale University Faculty of Medicine,  
Department of Pathology, Denizli, Türkiye

## PURPOSE

To compare the safety and diagnostic yield of two ultrasound (US)-guided percutaneous renal biopsy (PRB) approaches, lateral to medial and medial to lateral, which differ in access route, muscle groups traversed, and cortical targets.

## METHODS

This retrospective study included 490 patients (mean age:  $38.2 \pm 21.2$  years; 267 men, 223 women) who underwent US-guided PRB between 2019 and 2024 and had abdominal computed tomography (CT)/magnetic resonance imaging (MRI) within 1 year. At the left kidney lower pole level (L3–L4), anterior–posterior thicknesses of the traversed muscle groups were measured on CT/MRI. Complications were classified according to the Society of Interventional Radiology guidelines. Diagnostic yield was categorized as optimal ( $\geq 12$  glomeruli), suboptimal ( $\geq 3$  glomeruli), and pathologist based (diagnostic according to final pathology assessment). Group comparisons were performed using the chi-square test, Fisher's exact test, and t-test.

## RESULTS

In 490 PRBs (237 lateral to medial, 253 medial to lateral), the medial-to-lateral approach, despite traversing thicker muscles (35.7 vs. 11.5 mm,  $P = 0.001$ ), produced smaller hematomas (8.6 vs. 17.3 mm,  $P = 0.001$ ) with similar complication rates (major: 3.6% vs. 3.4%,  $P = 0.913$ ; minor: 36% vs. 33.8%,  $P = 0.608$ ). Diagnostic adequacy was comparable, but optimal yield was higher with the medial-to-lateral route (85.0% vs. 73.0%,  $P = 0.001$ ).

## CONCLUSION

Both approaches demonstrated comparable safety. However, the medial-to-lateral route was associated with smaller hematomas and a higher proportion of optimal biopsies from the lateral cortex, but suboptimal and pathologist-based adequacy remained high in both techniques.

## CLINICAL SIGNIFICANCE

When standard lower pole lateral cortex biopsy is not feasible due to cortical scarring, cysts, overlying skin lesions, or anatomic limitations—especially in patients for whom contralateral biopsy is not possible (e.g., solitary or ectopic pelvic kidney, severe unilateral hydronephrosis)—alternative cortical targets must be used. Understanding how different access routes and muscle pathways influence hemorrhage control and diagnostic yield helps operators choose the safest and most effective technique in these situations.

## KEYWORDS

Percutaneous renal biopsy, diagnostic yield, complications, muscle thickness, cortical targeting

Corresponding author: Kadir Han Alver

E-mail: [kadirhanalver@gmail.com](mailto:kadirhanalver@gmail.com)

Received 16 October 2025; revision requested 27 October 2025; accepted 21 November 2025.



Epub: 08.12.2025

Publication date:

DOI: 10.4274/dir.2025.253699

**P**ercutaneous renal biopsy (PRB) is a key procedure for diagnosing kidney disease, assessing prognosis, and guiding treatment. It is typically performed in patients with substantial proteinuria, hematuria, declining renal function, or suspected systemic disease involvement such as lupus or amyloidosis.<sup>1</sup> Although computed tomography (CT) guidance may be used in selected situations, ultrasound (US) is the preferred modality due to its re-

al-time visualization, lack of radiation, lower cost, and relatively short procedure time. When combined with spring-loaded core biopsy systems, US-guided PRB provides high diagnostic yield with an established safety profile.<sup>2</sup>

According to the Society of Interventional Radiology (SIR) and the Cardiovascular and Interventional Radiological Society of Europe (CIRSE), the standard technique for native kidney biopsy is a tangential medial-to-lateral approach targeting the lower pole lateral cortex, corresponding to Brödel's avascular zone, which provides a favorable balance between diagnostic yield and safety.<sup>3,4</sup> However, this pathway may not be feasible in cases such as asymmetric cortical thinning, large or multiple cysts, overlying skin lesions, or difficulty achieving optimal patient positioning. In these situations, particularly when contralateral biopsy is not possible (e.g., solitary or ectopic pelvic kidney, severe unilateral hydronephrosis, or extensive nephrolithiasis), biopsy may need to target alternative cortical regions via different anatomical routes. Although recent technical perspectives

suggest that any cortical region can be safely sampled if a tangential trajectory is maintained to avoid medullary and sinus injury, this assumption has not been systematically evaluated.<sup>5</sup> To date, no study has assessed whether differences in cortical target or the muscle groups traversed affect the safety or diagnostic performance of PRB.

At Pamukkale University Faculty of Medicine, Department of Interventional Radiology, two interventional radiologists, each with over 10 years of experience, routinely performed PRBs using different but consistent techniques, reflecting their procedural training and background. One radiologist used the standard medial-to-lateral approach, targeting the lower pole lateral cortex, whereas the other employed a lateral-to-medial approach, targeting the medial cortex. This systematic variation in cortical target, muscle pathway, and access route created a natural and unique comparison setting, enabling us to retrospectively evaluate how these technical differences influence safety and diagnostic yield, addressing a previously unexplored gap in the literature.

## Methods

### Patient selection

This retrospective study was approved by the Pamukkale University Ethical Committee of Non-Invasive Clinical Research (approval number: E-60116787-020-703301, date: 10.06.2025), and informed consent was waived. Patients were eligible if they underwent US-guided left PRB and had abdominal CT or magnetic resonance imaging (MRI) within 1 year of the procedure. Among the 716 PRBs performed between January 2019 and December 2024, patients were excluded for renal mass biopsy ( $n = 32$ ), CT-guided biopsy ( $n = 7$ ), transplanted kidney biopsy ( $n = 34$ ), absence of CT/MRI within 1 year ( $n = 84$ ), and renal orientation anomalies impairing cortical or trajectory assessment ( $n = 9$ ). Additional exclusions included resident-performed procedures ( $n = 13$ ), 16-gauge needle use ( $n = 10$ ), non-coaxial technique ( $n = 14$ ), incomplete 24-hour follow-up data ( $n = 11$ ), and right kidney biopsies ( $n = 12$ ). The final cohort consisted of 490 patients, comprising Group 1 (lateral-to-medial approach targeting the medial cortex;  $n = 237$ ; mean age:  $38 \pm 20.9$  years; 129 men) and Group 2 (medial-to-lateral approach targeting the lateral cortex;  $n = 253$ ; mean age:  $37.9 \pm 21.4$  years; 138 men) (Figure 1).

### Prebiopsy preparation

On the day of the procedure, all patients underwent laboratory evaluation. Biopsy was performed only if the platelet count was  $> 50,000/\text{mL}$ , the international normalized ratio was  $< 1.5$ , and hemoglobin was  $> 8 \text{ g/dL}$ .<sup>5</sup> Antiplatelet and anticoagulant medications were reviewed and adjusted (temporary discontinuation, bridging when indicated, and post-biopsy resumption) in accordance with SIR and CIRSE guidelines.<sup>4,6</sup> Because uncontrolled hypertension increases bleeding risk, biopsy proceeded only when blood pressure was  $< 160/90 \text{ mmHg}$ ; otherwise, antihypertensive optimization and rescheduling were performed.<sup>1,7</sup>

### Biopsy procedure

All biopsies were performed under real-time US guidance (ACUSON Sequoia, Siemens Healthineers, Mountain View, CA, USA; Aplio 500, Toshiba Medical Systems, Tokyo, Japan) using 1.5–6.0-MHz convex probes, with patients in the prone position under sterile conditions. Due to its more accessible position, the left kidney was consistently targeted, with all procedures guided sonographically in the transverse plane. Local anesthesia was provided using 10–20 mL of 1%–2% lidocaine. Two interventional radiologists, each with over 10 years of experience and more than 1,000 prior PRBs, performed the procedures using different but consistent approaches based on training preference. In Group 1, the biopsy was performed via a lateral skin entry, traversing the posterolateral abdominal wall muscles (latissimus dorsi, external oblique, internal oblique, transversus abdominis) to target the lower pole medial cortex (Figure 2). In Group 2, a medial skin entry was used, traversing the paravertebral muscles (multifidus, erector spinae, quadratus lumborum) to reach the lower pole lateral cortex (Figure 3). Patient allocation between the two groups was entirely random, as biopsies were performed by whichever radiologist was on duty on the day of the procedure. A coaxial technique was used in all cases: a 17-gauge introducer needle was advanced to the renal capsule, through which a 15-cm, 18-gauge spring-loaded core needle (Max-core, Bard Biopsy Systems, Tempe, Arizona) with a penetration depth of 22 mm and a sample notch of 18 mm was used to obtain two tissue samples with a tangential cortical trajectory. If bleeding occurred through the coaxial introducer, temporary tract tamponade was performed by reinserting the stylet, and persistent bleeding was managed with autologous blood clot or absorbable

### Main points

- This study directly compared two ultrasound-guided percutaneous renal biopsy techniques—lateral to medial and medial to lateral—that differ in cortical targets, routes, and muscle pathways. The medial-to-lateral approach traverses the paravertebral muscles (multifidus, erector spinae, quadratus lumborum) to sample the lower pole lateral cortex, whereas the lateral-to-medial approach passes through the posterolateral abdominal wall muscles (latissimus dorsi, external and internal obliques, transversus abdominis) to reach the lower pole medial cortex.
- Safety was comparable between approaches, with similar rates of minor and major complications within Society of Interventional Radiology guideline thresholds.
- The medial-to-lateral approach, which traverses thicker paravertebral muscles, resulted in smaller non-transfusion-requiring perirenal hematomas.
- Optimal diagnostic yield ( $\geq 12$  glomeruli) was higher with the medial-to-lateral approach, whereas suboptimal yield ( $\geq 3$  glomeruli) and pathologist-based adequacy remained high in both techniques.
- This is the first study to systematically evaluate how cortical targets and muscle pathways affect biopsy outcomes, providing practical guidance for cases in which standard lower pole lateral cortex access cannot be used.

gelatin sponge (Spongostan, Ethicon, NJ, USA). Specimens were transported in phosphate-buffered saline for light microscopy (LM), immunofluorescence (IF), and electron microscopy (EM). On-site adequacy assessment was not performed due to the lack of cytotechnologist support. Local anesthesia was standard, and conscious sedation was used selectively in pediatric or anxious patients with anesthesiology support.<sup>8</sup>

Post-biopsy monitoring

After biopsy and dressing, patients were kept supine with a sandbag under the left kidney for 6 hours and observed for 24 hours. At the 6<sup>th</sup> hour, follow-up renal US was performed in the interventional radiology suite, and the presence and maximum size of biopsy-related hemorrhage were recorded. Hemoglobin was assessed at the 6<sup>th</sup> hour and repeated at 24 hours before discharge. Vital signs were monitored every 30 minutes for 2 hours, hourly for 4 hours, and every 2 hours thereafter. Patients were observed for hematuria and bleeding-related symptoms (flank pain, dizziness, vomiting, presyncope). If major bleeding was suspected—macrohematuria, hypotension, tachycardia, or large perirenal/retroperitoneal hematoma—non-contrast CT was performed, followed by contrast-enhanced CT or angiography when needed. Patients who were hemodynamically stable and asymptomatic without ongoing hemoglobin decline were discharged after 24 hours with return precautions.<sup>1,5,7</sup>

In accordance with the SIR guidelines, complications were classified as major (requiring transfusion, radiologic/surgical intervention, or associated with renal obstruction/failure, sepsis, permanent sequelae, or death) or minor (transient hematuria or small perirenal/retroperitoneal hematomas resolving spontaneously without transfusion or extended hospitalization).<sup>9</sup>

Radiologic and pathologic evaluation

During pre-procedural US, the long-axis length and parenchymal thickness of the target kidney were measured. At the lower pole level (typically L3–L4), the anterior–posterior thickness of the muscle groups along the biopsy path was measured on CT/MRI. In the lateral-to-medial approach (Group 1), this included the posterolateral abdominal wall muscles (external oblique, internal oblique, transversus abdominis, latissimus dorsi), whereas in the medial-to-lateral approach (Group 2), it included the paravertebral muscles (multifidus, erector spinae, quadratus lumborum). Multiple measurements were

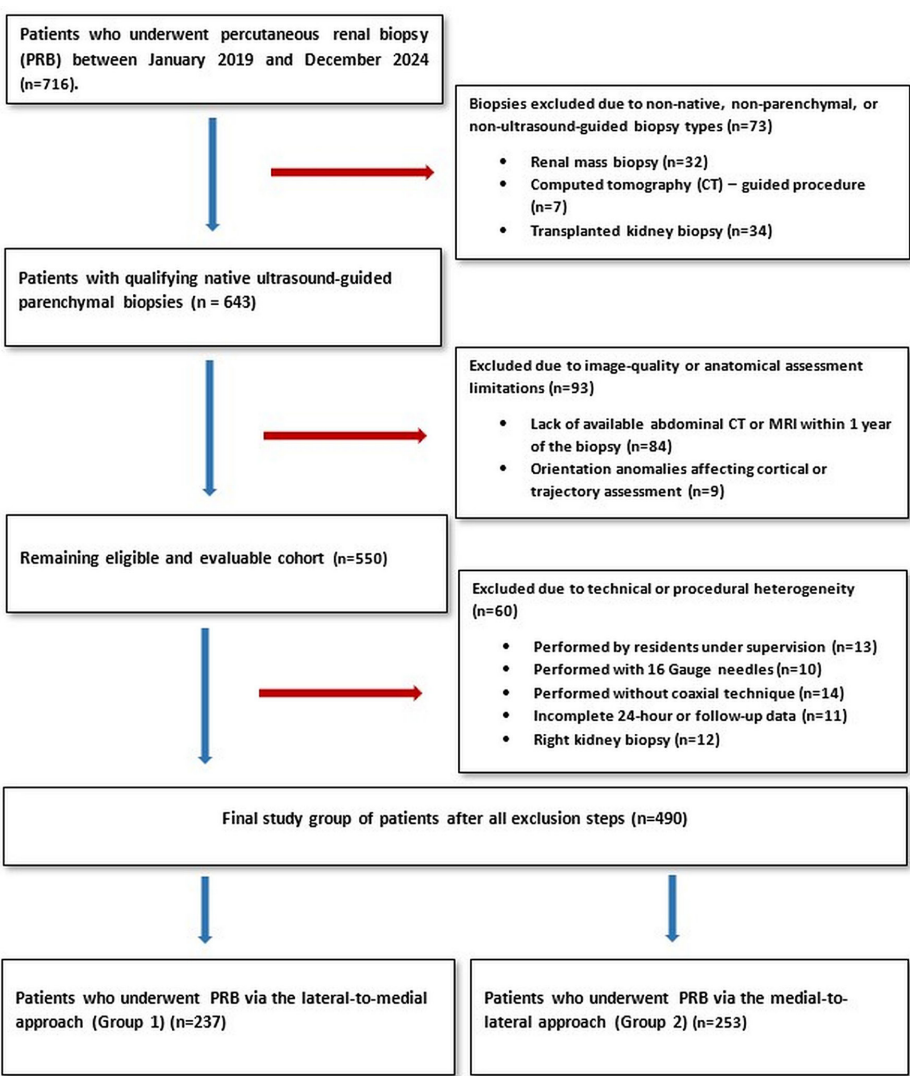


Figure 1. Flowchart of study population. MRI, magnetic resonance imaging.

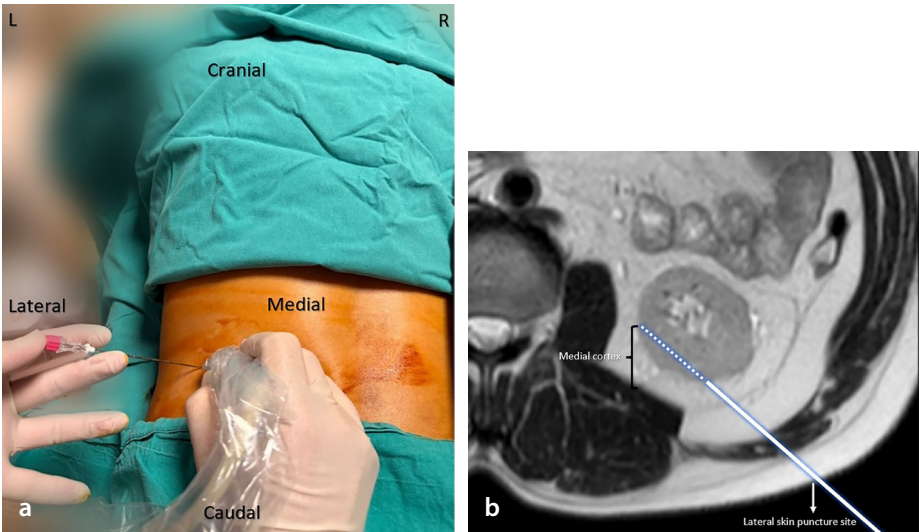


Figure 2. Lateral-to-medial approach for left kidney biopsy. (a) Intra-procedural photograph, obtained under sterile conditions with the patient in the prone position, demonstrating lateral skin entry of a 17G introducer needle under ultrasound guidance to target the medial cortex. (b) Illustration of the renal parenchymal biopsy performed using the cortical–tangential technique, with traversal of the posterolateral abdominal wall muscles and targeting of the medial cortex (L, left; R, right; G, gauge).



obtained across each muscle group at this level, and mean values were used for analysis. Demographics, biopsy approach and operator, hemoglobin values, sonographic findings, histopathology, glomerular counts, and complications were retrieved from electronic records and Picture Archiving and Communication Systems.

All specimens were evaluated by a nephropathologist with over 15 years of experience. Consistent with the literature, biopsies were categorized based on total glomerular count across LM, IF, and EM.<sup>10,11</sup>

- **Group A (optimal):**  $\geq 12$  glomeruli total ( $\geq 10$  for LM +  $\geq 1$  for IF +  $\geq 1$  for EM),
- **Group B (suboptimal):**  $\geq 3$  glomeruli total, with at least one evaluable glomerulus in each modality but not meeting the Group A criteria, and
- **Group C (inadequate):**  $< 3$  glomeruli or missing required modalities.

Diagnostic yield was defined as follows:

1. **Optimal yield:** Proportion of Group A biopsies ( $\geq 12$  glomeruli),
2. **Suboptimal yield:** Proportion of biopsies with  $\geq 3$  glomeruli (Groups A + B), and
3. **Pathologist-based yield:** Biopsies deemed diagnostic in the final report, regardless of glomerular count.

Yield ratios were calculated as diagnostic biopsies divided by total biopsies in each group.

Statistical analysis

Statistical analyses were conducted using SPSS version 25.0 (IBM Corp., Armonk, NY, USA). Categorical variables were reported as counts and percentages and continuous variables as mean  $\pm$  standard deviation. Normality was assessed using the Shapiro–Wilk test.

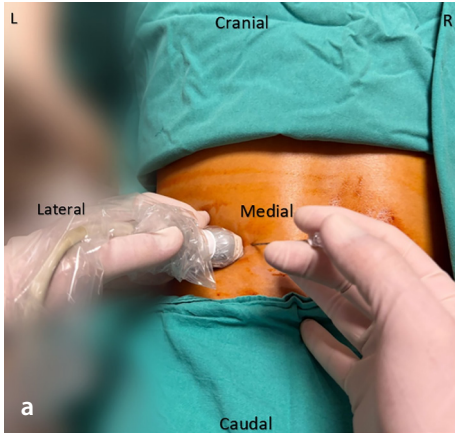


**Figure 3.** Medial-to-lateral approach for left kidney biopsy. (a) Intra-procedural photograph, obtained under sterile conditions with the patient in the prone position, demonstrating medial skin entry of a 17G introducer needle under ultrasound guidance to target the lateral cortex. (b) Illustration of the renal parenchymal biopsy performed using the cortical–tangential technique, with traversal of the paravertebral muscles and targeting of the lateral cortex (L, left; R, right; G, gauge).

Patients were grouped according to the biopsy approach (Group 1: lateral to medial; Group 2: medial to lateral). Diagnostic yield and major/minor complications were compared using chi-square or Fisher's exact tests. Total muscle thickness, total glomerular count, hemoglobin change (baseline vs. 6 and 24 hours), and hematoma size were compared using the independent-samples t-test or Mann–Whitney U test, depending on the distribution. A *P* value  $< 0.05$  was considered statistically significant.

Results

A total of 490 patients were included (mean age:  $38.2 \pm 21.2$  years; 267 men, 223 women), comprising 237 who underwent the lateral-to-medial approach (Group 1) and 253 who underwent the medial-to-lateral approach (Group 2). The most common histopathological diagnosis was focal segmental glomerulosclerosis (79/490, 16.1%), followed by membranous nephropathy (48/490, 9.8%) and lupus nephritis (39/490,

8.0%). The full diagnostic distribution is summarized in Table 1.

Baseline demographic characteristics, renal long-axis length, parenchymal thickness, and mean hemoglobin decline at both the 6<sup>th</sup> and 24<sup>th</sup> hours were comparable between the two groups (all *P*  $> 0.05$ ). However, muscle thickness along the biopsy tract differed substantially, being significantly lower in Group 1 than in Group 2 ( $11.5 \pm 4.2$  vs.  $35.7 \pm 10.9$  mm, *P* = 0.001) (Table 2).

The suboptimal diagnostic yield ( $\geq 3$  glomeruli) was similarly high in Group 1 and Group 2 (95.4% vs. 95.3%, *P* = 0.958), and pathologist-based adequacy was also comparable (96.6% vs. 98.0%, *P* = 0.335). However, the proportion of biopsies achieving  $\geq 12$  glomeruli (optimal diagnostic yield) was significantly higher in Group 2 (85.0% vs. 73.0%, *P* = 0.001) (Table 2).

**Table 1.** Distribution of histopathological diagnoses by biopsy approach

		Lateral-to-medial approach (Group 1) (n = 237)	Medial-to-lateral approach (Group 2) (n = 253)	Total	Percentage (%)
1	Focal segmental glomerulosclerosis	38	41	79	16.1%
2	Membranous nephropathy	23	25	48	9.8%
3	Lupus nephritis	16	23	39	8.0%
4	Crescentic glomerulonephritis	15	18	33	6.7%
5	Immunoglobulin A nephropathy	15	14	29	5.9%
6	Acute interstitial nephritis	14	13	27	5.5%
7	Chronic glomerulonephritis	12	14	26	5.3%
8	Henoch–Schönlein purpura nephritis	13	12	25	5.1%

**Table 1. Continued**

		Lateral-to-medial approach (Group 1) (n = 237)	Medial-to-lateral approach (Group 2) (n = 253)	Total	Percentage (%)
9	Normal histology/no specific pathology	12	13	25	5.1%
10	Membranoproliferative glomerulonephritis type I	10	7	17	3.5%
11	Diabetic nephropathy	7	8	15	3.1%
12	Serum amyloid A protein amyloidosis	5	9	14	2.9%
13	C3 glomerulopathy	6	7	13	2.7%
14	Non-diagnostic	8	5	13	2.7%
15	mesangial hypercellularity ± glomerulosclerosis, not otherwise specified	5	6	11	2.2%
16	Chronic interstitial nephritis	5	6	11	2.2%
17	Minimal change disease	7	4	11	2.2%
18	Vasculitis	6	1	7	1.4%
19	Acute tubular necrosis	1	5	6	1.2%
20	Hypertensive nephropathy	2	4	6	1.2%
21	Small-vessel vasculitis	4	1	5	1.0%
22	Postinfectious glomerulonephritis	2	3	5	1.0%
23	Diffuse proliferative glomerulonephritis	3	1	4	0.8%
24	Chronic pyelonephritis	1	2	3	0.6%
25	Myeloma cast nephropathy	0	3	3	0.6%
26	Immunoglobulin light chain amyloidosis	0	2	2	0.4%
27	Microscopic polyangiitis	1	1	2	0.4%
28	Diffuse large B-cell lymphoma	1	1	2	0.4%
29	Thrombotic microangiopathy	1	1	2	0.4%
30	Isolated Bowman's capsule thickening	0	1	1	0.2%
31	Fibrillary glomerulonephritis	1	0	1	0.2%
32	Isolated glomerulomegaly	1	0	1	0.2%
33	Granulomatosis with polyangiitis	0	1	1	0.2%
34	Lymphoplasmacytic lymphoma	1	0	1	0.2%
35	Nephrocalcinosis	1	0	1	0.2%
36	Necrotizing granulomatous inflammation	0	1	1	0.2%
	Total	237	253	490	100.0%

**Table 2.** Procedural characteristics, diagnostic yield, and complications in Group 1 (lateral to medial) and Group 2 (medial to lateral) approaches

	Lateral-to-medial approach (Group 1) (n = 237)	Medial-to-lateral approach (Group 2) (n = 253)	P value	Test
Age (years)	38 ± 20.9	37.9 ± 21.4	0.693	t
Gender (men/women)	(129/108)	(138/115)	0.980	χ <sup>2</sup>
Renal long-axis length (mm)	109.3 ± 13	109.5 ± 12.9	0.830	t
Renal parenchymal thickness (mm)	16.2 ± 2.8	16.3 ± 3.1	0.801	t
Total muscle thickness traversed (mm)	11.5 ± 4.2	35.7 ± 10.9	<b>0.001</b>	t
Mean hemoglobin decline (Prebiopsy - 6 <sup>th</sup> hour post-biopsy) (g/dL)	0.44 ± 0.79	0.37 ± 0.63	0.297	t
Mean hemoglobin decline (Prebiopsy - 24 <sup>th</sup> hour post-biopsy) (g/dL)	0.34 ± 0.84	0.33 ± 0.78	0.980	t
Mean number of glomeruli in biopsies	17.3 ± 10.9 (n = 237)	18.4 ± 10.3 (n = 253)	0.243	t

	Lateral-to-medial approach (Group 1) (n = 237)	Medial-to-lateral approach (Group 2) (n = 253)	P value	Test
Optimal ( $\geq 12$ glomeruli)	21.5 $\pm$ 9.8 (n = 173)	20.9 $\pm$ 9.2 (n = 215)	0.511	t
Suboptimal ( $\geq 3$ and $< 12$ glomeruli)	7.0 $\pm$ 1.9 (n = 53)	6.2 $\pm$ 1.6 (n = 26)	0.058	t
Inadequate ( $< 3$ glomeruli)	1.5 $\pm$ 1.4 (n = 11)	1.7 $\pm$ 1.2 (n = 12)	0.724	f
Optimal diagnostic yield*	73.0%	85.0%	<b>0.001</b>	$\chi^2$
Suboptimal diagnostic yield*	95.4%	95.3%	0.958	$\chi^2$
Diagnostic yield with pathology opinion	96.6%	98.0%	0.335	$\chi^2$
Minor complications	80/237 (33.8%)	91/253 (36%)	0.608	$\chi^2$
Maximum perirenal hematoma size (minor, non-transfusion requiring) (mm)	17.3 $\pm$ 12.6	8.6 $\pm$ 8.9	<b>0.001</b>	t
Major complications	8/237 (3.4%)	9/253 (3.6%)	0.913	$\chi^2$
Total complications	88/237 (37.1%)	100/253 (39.5%)	0.586	$\chi^2$

t: Student's t-test for independent samples;  $\chi^2$ , chi-square test; f, Fisher's exact test; \*, optimal diagnostic yield was calculated as the proportion of biopsies with  $\geq 12$  glomeruli (O) among all biopsies (O + SO + IA). Suboptimal diagnostic yield was calculated as the proportion of biopsies with  $\geq 3$  glomeruli (O + SO) among all biopsies (O + SO + IA). O: Optimal ( $\geq 12$  glomeruli); SO, suboptimal (3–11 glomeruli); IA, inadequate ( $< 3$  glomeruli).

Overall, minor and major complication rates were also similar between Group 1 and Group 2 (37.1% vs. 39.5%,  $P = 0.586$ ; 33.8% vs. 36.0%,  $P = 0.608$ ; and 3.4% vs. 3.6%,  $P = 0.913$ , respectively). The most common minor and major complications were non-transfusion-requiring perirenal hematoma (29.5% vs. 30.4%) and hemorrhage requiring transfusion (1.3% vs. 2.0%), respectively (Figures 4 and 5). Although the frequency of perirenal hematoma was similar, hematoma size was significantly smaller in Group 2 (8.6  $\pm$  8.9 vs. 17.3  $\pm$  12.6 mm,  $P = 0.001$ ). Detailed complication subtypes are presented in Table 3.

## Discussion

This study compared medial-to-lateral and lateral-to-medial PRB approaches, showing similar overall safety but notable differences related to the muscle thickness and cortical region sampled. The medial-to-lateral approach traversed thicker paravertebral muscles (35.7  $\pm$  10.9 vs. 11.5  $\pm$  4.2 mm,  $P = 0.001$ ) and was associated with smaller non-transfusion-requiring perirenal hematomas (8.6  $\pm$  8.9 vs. 17.3  $\pm$  12.6 mm,  $P = 0.001$ ). This suggests that thicker, more compact muscle groups and a shorter retroperitoneal course may provide a tamponade effect that limits hematoma expansion, whereas thinner posterolateral muscles may permit greater spread. Although bleeding originates in the kidney, similar principles have been described in other contexts. In subcapsular liver lesion biopsies, traversing a short segment of normal parenchyma is recommended so that the surrounding tissue can help compress and limit bleeding.<sup>12</sup> Likewise, rectus sheath and iliopsoas hematomas often remain self-contained due to the natu-

**Table 3. Minor and major complications following percutaneous renal biopsy in Group 1 (lateral to medial) and Group 2 (medial to lateral) approaches**

Complication	Lateral-to-medial approach (Group 1)		Medial-to-lateral approach (Group 2)		Total	
	(n = 237)		(n = 253)		(n = 490)	
	(n)	(%)	(n)	(%)	(n)	(%)
Perirenal hematoma (non-transfusion requiring)	70	29.5%	77	30.4%	147	30.0%
Self-limiting discomfort symptoms	4	1.7%	6	2.4%	10	2.0%
Macroscopic hematuria	5	2.1%	6	2.4%	11	2.2%
Vasovagal reaction	1	0.4%	1	0.4%	2	0.4%
Bladder hematoma	0	0.0%	1	0.4%	1	0.2%
<b>Minor complications</b>	<b>80</b>	<b>33.8%</b>	<b>91</b>	<b>36.0%</b>	<b>171</b>	<b>34.9%</b>
Hemorrhage requiring transfusion (perirenal or retroperitoneal)	3	1.3%	5	2.0%	8	1.6%
Subcapsular hemorrhage requiring transfusion	1	0.4%	0	0.0%	1	0.2%
Arteriovenous fistula	1	0.4%	2	0.8%	3	0.6%
Arteriovenous fistula and pseudoaneurysm	2	0.8%	2	0.8%	4	0.8%
Death	1	0.4%	0	0.0%	1	0.2%
<b>Major complications</b>	<b>8</b>	<b>3.4%</b>	<b>9</b>	<b>3.6%</b>	<b>17</b>	<b>3.5%</b>
<b>Total complications</b>	<b>88</b>	<b>37.1%</b>	<b>100</b>	<b>39.5%</b>	<b>188</b>	<b>38.4%</b>

ral pressure of muscular compartments.<sup>13,14</sup> Additionally, greater muscle thickness along nephrostomy catheter tracts has been associated with reduced catheter displacement, suggesting that deeper musculature has a stabilizing effect.<sup>15</sup> Although no study has directly evaluated the influence of muscle layers on bleeding after renal biopsy, these parallels support the plausibility that thicker muscle groups may similarly help constrain post-biopsy hemorrhage.

Major complications occurred at similar rates in the lateral-to-medial and me-

dial-to-lateral groups (3.4% vs. 3.6%,  $P = 0.913$ ), remaining below the  $< 5\%$  threshold recommended by SIR for PRB.<sup>3</sup> These low rates likely reflect strict adherence to guideline-based anticoagulation management,<sup>4–6</sup> optimization of blood pressure,<sup>16</sup> performance in a high-volume tertiary center,<sup>17</sup> use of 18-gauge needles<sup>18</sup> and a coaxial technique,<sup>19</sup> tract tamponade/embolization when indicated,<sup>20</sup> and maintenance of a cortical-tangential trajectory.<sup>11,21,22</sup> Minor complications were also comparable between groups (33.8% vs. 36.0%,  $P = 0.608$ ), with



**Figure 4.** Examples of perirenal hemorrhage following biopsy using the lateral-to-medial approach. (a) Transverse non-contrast abdominal computed tomography (CT) images of a 45-year-old male patient who underwent percutaneous renal biopsy (PRB) for proteinuria, showing perirenal hemorrhage (yellow arrow) at the level corresponding to the needle entry site into the left kidney. (b) Axial non-contrast abdominal CT images obtained after PRB in a 51-year-old female patient being followed for vasculitis to assess renal involvement, demonstrating minimal perirenal hemorrhage (yellow arrow).

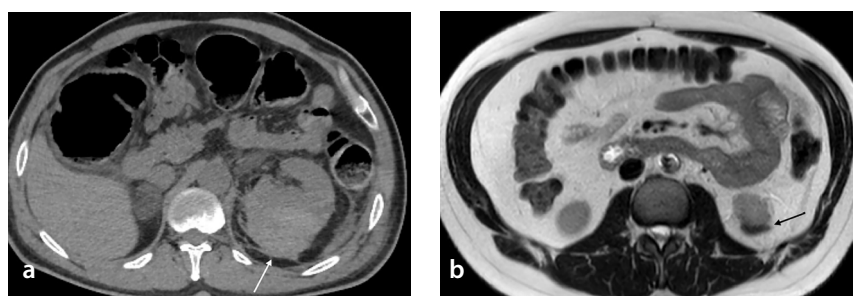


**Figure 5.** Examples of perirenal hemorrhage following biopsy using the medial-to-lateral approach. (a) Axial non-contrast abdominal computed tomography images of a 37-year-old male patient who underwent parenchymal renal biopsy (PRB) for nephrotic syndrome, showing perirenal hemorrhage (white arrow) in continuity with the kidney at its posterior aspect. (b) Axial non-fat-suppressed T2-weighted magnetic resonance imaging of a 45-year-old male patient who underwent PRB for acute kidney injury, demonstrating minimal hypointense perirenal hemorrhage (black arrow).

non-transfusion-requiring perirenal hematomas being the most frequent (29.5% vs. 30.4%,  $P = 0.792$ ). Although these rates may appear high relative to the broad literature estimates (1.3%–33.3%),<sup>7</sup> they align with studies performing routine post-biopsy US in all patients, which report hematoma detection rates of 33%–58%.<sup>23–25</sup> This suggests that perirenal hematomas are likely under-recognized in studies that image only symptomatic patients.

Most studies describe targeting the lower pole in PRB without specifying cortical orientation, with only a few explicitly mentioning the lower pole lateral cortex.<sup>23,24</sup> However, none evaluate whether sampling the medial cortex affects diagnostic outcomes, making this the first study to systematically assess this distinction in routine practice. Suboptimal diagnostic yield ( $\geq 3$  glomeruli) (95.4% vs. 95.3%,  $P = 0.958$ ) and pathologist-based diagnostic adequacy (96.6% vs. 98.0%,  $P = 0.335$ ) were similar between groups, as were mean glomerular counts across optimal ( $21.5 \pm 9.8$  vs.  $20.9 \pm 9.2$ ,  $P = 0.511$ ), suboptimal ( $7.0 \pm 1.9$  vs.  $6.2 \pm 1.6$ ,  $P = 0.058$ ), and inadequate ( $1.5 \pm 1.4$  vs.  $1.7 \pm 1.2$ ,  $P = 0.724$ ) biopsy cat-

egories. However, the proportion of optimal biopsies ( $\geq 12$  glomeruli) was lower in the lateral-to-medial approach (73.0% vs. 85.0%,  $P = 0.001$ ), below the 88% technical success benchmark recommended by SIR.<sup>3</sup> Although this difference may suggest that the cortical region targeted could influence tissue yield, we emphasize that this remains speculative, as no histopathologic study has compared glomerular density between the medial and lateral cortices. Although SIR recommends obtaining  $\geq 10$  glomeruli in diffuse and  $\geq 20$  in focal diseases, no universally accepted adequacy threshold exists for native kidney biopsies.<sup>3,26–31</sup> Adequacy assessment varies among nephropathologists, and the required number of glomeruli depends on disease distribution (diffuse vs. focal); the necessity of LM, IF, and EM for all cases also remains debated.<sup>26,32,33</sup> Classification systems such as that developed by Geldenhuys et al.,<sup>10</sup> although useful for quality benchmarking, may not fully reflect real-world diagnostic decision-making. In our study, although an optimal yield difference was observed, both approaches achieved high suboptimal and pathologist-based diagnostic adequacy, suggesting that overall diagnostic reliability

remained clinically acceptable. Nevertheless, when medial cortical sampling is required, operators may consider yield-enhancing strategies such as using a needle with a larger gauge and obtaining  $\geq 3$  cores<sup>34</sup> or coordinating with an on-site or bedside pathologist.<sup>5</sup> Finally, although one autopsy study compared glomerular distribution between juxtamedullary and subcapsular regions,<sup>35</sup> no nephrectomy or autopsy study has compared glomerular density between the medial and lateral cortices. Future comparative studies may clarify whether intrinsic cortical differences contribute to the yield patterns observed here.

Our study has limitations. First, it was a single-center, retrospective analysis, and selection and information bias may have been introduced. Second, muscle thickness measurements were performed at the lower pole level on CT/MRI, but the biopsy needle trajectory may not have perfectly matched the measurement plane. However, the marked difference in muscle thickness between approaches and the exclusion of cases with orientation anomalies likely minimized the impact of this limitation. Because the traversed muscle groups differed substantially, procedure-related pain may also have differed between approaches; however, pain assessment (e.g., visual analog scale scoring) was not available due to the retrospective design. Additionally, procedures were performed by two interventional radiologists, introducing potential operator-related variability. Nevertheless, both had  $> 10$  years of experience and had performed  $> 1,000$  biopsies each, consistently using their respective techniques, which likely reduced skill-based differences. Prospective, multicenter, randomized studies are needed to validate these findings and further clarify the influence of approach-related factors on biopsy outcomes.

In conclusion, this study—the first to compare how different access routes, muscle pathways, and cortical targets influence PRB performance—demonstrated that both approaches are safe with acceptable complication rates. The medial-to-lateral approach, which traverses thicker paravertebral muscles to sample the lateral cortex, resulted in smaller hematomas and a higher optimal diagnostic yield. Although suboptimal and pathologist-based adequacy were similarly high in both groups, operators should recognize the slightly lower optimal yield when sampling the medial cortex and may adjust techniques accordingly.



## Footnotes

## Conflict of interest disclosure

The authors declared that there is no conflict of interest.

## References

1. Granata A, Distefano G, Pesce F, et al. Performing an ultrasound-guided percutaneous needle kidney biopsy: an up-to-date procedural review. *Diagnostics (Basel)*. 2021;11(12):2186. [\[Crossref\]](#)
2. MacGinley R, Champion De Crespigny PJ, Gutman T, et al. KHA-CARI Guideline recommendations for renal biopsy. *Nephrology (Carlton)*. 2019;24(12):1205-1213. [\[Crossref\]](#)
3. Sheth RA, Baerlocher MO, Connolly BL, et al. Society of Interventional Radiology Quality Improvement Standards on percutaneous needle biopsy in adult and pediatric patients. *J Vasc Interv Radiol*. 2020;31(11):1840-1848. [\[Crossref\]](#)
4. Veltri A, Bargellini I, Giorgi L, Almeida PAMS, Akhan O. CIRSE Guidelines on percutaneous needle biopsy (PNB). *Cardiovasc Intervent Radiol*. 2017;40(10):1501-1513. [\[Crossref\]](#)
5. Shyn PB, Patel MD, Itani M, et al. Image-guided renal parenchymal biopsies- how we do it. *Abdom Radiol (NY)*. 2025;50(6):2595-2605. [\[Crossref\]](#)
6. Davidson JC, Rahim S, Hanks SE, et al. Society of Interventional Radiology Consensus Guidelines for the periprocedural management of thrombotic and bleeding risk in patients undergoing percutaneous image-guided interventions-part I: review of anticoagulation agents and clinical considerations: endorsed by the Canadian Association for Interventional Radiology and the Cardiovascular and Interventional Radiological Society of Europe. *J Vasc Interv Radiol*. 2019;30(8):1155-1167. [\[Crossref\]](#)
7. Schnuelle P. Renal biopsy for diagnosis in kidney disease: indication, technique, and safety. *J Clin Med*. 2023;12(19):6424. [\[Crossref\]](#)
8. Patatas K, Koukkouli A. The use of sedation in the radiology department. *Clin Radiol*. 2009;64(7):655-663. [\[Crossref\]](#)
9. Khalilzadeh O, Baerlocher MO, Shyn PB, et al. Proposal of a new adverse event classification by the Society of Interventional Radiology Standards of Practice Committee. *J Vasc Interv Radiol*. 2017;28(10):1432-1437. [\[Crossref\]](#)
10. Geldenhuys L, Nicholson P, Sinha N, et al. Percutaneous native renal biopsy adequacy: a successful interdepartmental quality improvement activity. *Can J Kidney Health Dis*. 2015;2:8. [\[Crossref\]](#)
11. Liu B, O'Dell M, Flores M, et al. CT-guided native medical renal biopsy: cortical tangential versus non-tangential approaches-a comparison of efficacy and safety. *Radiology*. 2017;283(1):293-299. [\[Crossref\]](#)
12. Potretzke TA, Saling LJ, Middleton WD, Robinson KA. Bleeding complications after percutaneous liver biopsy: do subcapsular lesions pose a higher risk? *AJR Am J Roentgenol*. 2018;211(1):204-210. [\[Crossref\]](#)
13. Allen M, Sevensma KE. Rectus Sheath Hematoma. In: *StatPearls*. StatPearls Publishing; 2025. Accessed July 28, 2025. [\[Crossref\]](#)
14. Kameda T, Fujita M, Takahashi I. Diagnosis of traumatic iliopsoas hematoma using point-of-care ultrasound. *Crit Ultrasound J*. 2011;3(1):59-61. [\[Crossref\]](#)
15. Ütebey AR, Aslan HS, Arslan M, et al. Predictive factors for spontaneous dislodgement of percutaneous nephrostomies for malignant ureteral obstruction. *Abdom Radiol (NY)*. 2025;50(9):4268-4282. [\[Crossref\]](#)
16. Kriegshauser JS, Patel MD, Young SW, Chen F, Eversman WG, Chang YH. Risk of bleeding after native renal biopsy as a function of preprocedural systolic and diastolic blood pressure. *J Vasc Interv Radiol*. 2015;26(2):206-212. [\[Crossref\]](#)
17. Tøndel C, Vikse BE, Bostad L, Svarstad E. Safety and complications of percutaneous kidney biopsies in 715 children and 8573 adults in Norway 1988-2010. *Clin J Am Soc Nephrol*. 2012;7(10):1591-1597. [\[Crossref\]](#)
18. Chunduri S, Whittier WL, Korbet SM. Adequacy and complication rates with 14- vs. 16-gauge automated needles in percutaneous renal biopsy of native kidneys. *Semin Dial*. 2015;28(2):E11-4. [\[Crossref\]](#)
19. Fung KFK, Cheng KK, Chan EY, Ma LTA, Cho HYD, Kan YLE. Percutaneous ultrasound-guided renal biopsies in a paediatric population: comparison of coaxial and non-coaxial techniques using 18-gauge core biopsy needles. *Pediatr Radiol*. 2022;52(12):2431-2437. [\[Crossref\]](#)
20. Strnad BS, Itani M, Middleton WD. Detection and management of bleeding in the setting of image-guided percutaneous needle biopsy. *Abdom Radiol (NY)*. 2022;47(8):2681-2696. [\[Crossref\]](#)
21. Patel MD, Phillips CJ, Young SW, et al. US-guided renal transplant biopsy: efficacy of a cortical tangential approach. *Radiology*. 2010;256(1):290-296. [\[Crossref\]](#)
22. Li Q, Lin X, Zhang X, Samir AE, Arellano RS. Imaging-related risk factors for bleeding complications of US-guided native renal biopsy: a propensity score matching analysis. *J Vasc Interv Radiol*. 2019;30(1):87-94. [\[Crossref\]](#)
23. Xu S, Xiong B, Lin S, Li Q, Wang L, Zhao W. Predictors of perirenal haematoma post-percutaneous ultrasound-guided renal biopsy. *J Int Med Res*. 2021;49(11):3000605211058377. [\[Crossref\]](#)
24. Li FF, Guan YX, Li TX, et al. Analysis of hemorrhage upon ultrasound-guided percutaneous renal biopsy in China: a retrospective study. *Int Urol Nephrol*. 2024;56(5):1713-1720. [\[Crossref\]](#)
25. Manno C, Strippoli GF, Arnesano L, et al. Predictors of bleeding complications in percutaneous ultrasound-guided renal biopsy. *Kidney Int*. 2004;66(4):1570-1577. [\[Crossref\]](#)
26. Liu B, O'Dell M, Flores M, et al. CT-guided native medical renal biopsy: cortical tangential versus non-tangential approaches-a comparison of efficacy and safety. *Radiology*. 2017;283(1):293-299. [\[Crossref\]](#)
27. Loupy A, Haas M, Roufosse C, et al. The Banff 2019 Kidney Meeting Report (I): updates on and clarification of criteria for T cell- and antibody-mediated rejection. *Am J Transplant*. 2020;20(9):2318-2331. [\[Crossref\]](#)
28. Constantin A, Brisson ML, Kwan J, Proulx F. Percutaneous US-guided renal biopsy: a retrospective study comparing the 16-gauge end-cut and 14-gauge side-notch needles. *J Vasc Interv Radiol*. 2010;21(3):357-61. [\[Crossref\]](#)
29. Ferguson C, Winters S, Jackson S, McToal M, Low G. A retrospective analysis of complication and adequacy rates of ultrasound-guided native and transplant non-focal renal biopsies. *Abdom Radiol N Y*. 2018;43(8):2183-2189. [\[Crossref\]](#)
30. Goldstein MA, Atri M, O'Malley M, et al. Nonfocal renal biopsies: adequacy and factors affecting a successful outcome. *J Comput Assist Tomogr*. 2013;37(2):176-182. [\[Crossref\]](#)
31. Wooldridge JT, Davis A, Fischer WG, Khalil MF, Zhang M, Afrouzian M. The impact of renal tissue procurement at bedside on specimen adequacy and best practices. *Am J Clin Pathol*. 2019;151(2):205-208. [\[Crossref\]](#)
32. Chang A, Gibson IW, Cohen AH, et al. A position paper on standardizing the nonneoplastic kidney biopsy report. *Clin J Am Soc Nephrol*. 2012;7(8):1365-1368. [\[Crossref\]](#)
33. Walker PD, Cavallo T, Bonsib SM; Ad Hoc Committee on Renal Biopsy Guidelines of the Renal Pathology Society. Practice guidelines for the renal biopsy. *Mod Pathol*. 2004;17(12):1555-1563. [\[Crossref\]](#)
34. Corapi KM, Chen JLT, Balk EM, Gordon CE. Bleeding complications of native kidney biopsy: a systematic review and meta-analysis. *Am J Kidney Dis*. 2012;60(1):62-73. [\[Crossref\]](#)
35. Kanzaki G, Tsuboi N, Utsunomiya Y, Ikegami M, Shimizu A, Hosoya T. Distribution of glomerular density in different cortical zones of the human kidney. *Pathol Int*. 2013;63(3):169-175. [\[Crossref\]](#)